

Final project

Topic: Automatic flat polyp detection in colonoscopy videos

1. Feature extraction

a). Edge features

a. Introduction

There are three types of edge patterns in colons:

- 1) Occlusion boundaries of ridges on the colon; these edges are deep, are more or less parallel and have large spacing
- 2) innominate grooves (colon commonly covered by parallel and narrow grooves, those grooves low contrast intensity) with parallel pattern
- 3) random lines.

Those three types of edge patterns are useful to detect flat lesions:

- 1) Ridge disruptions can signal flat lesions.
- 2) Innominate grooves disruptions can signal flat lesions. Moreover, flat lesions do not contain innominate grooves.
- 3) Random textures can signal flat lesions, so random lines that come from them can be part of a signal.

b. specularity removal

Before I try to detect edge pattern in colons, I should recolor specular regions because their strong edges confuse the feature choices used in texture analysis. Our method is to recolor specular regions by a deep neural network.

Specular regions are caused by reflections from the colon surface. The dispnet structure [1] allows us to build a neural network which inputs a frame with specular regions and outputs a frame without specular regions.

To train this neural network, I created a database including 256 frames without specularity recolored and 256 frames which have recolored specular regions. I extracted 256 frames from a colonoscopy video to use as training inputs. I used an app named Meitu[2], which is an image processing app which can cosmetically erase acne in the human face, to recolor specular regions. I obtained no specularity frames by this image processing app. Fig 1 shows the results of our neural network.

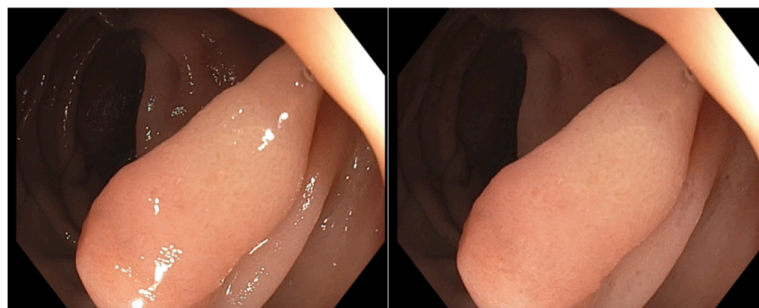


Figure 1: Polyp image from a colonoscopy video before (left) and after (right) specular reflection removal.

c. Random line detection

Next, I need to detect all the edge patterns. Since I aim to distinguish edges in lesions that are not more or less parallel from those in innominate grooves or ridges that are more or less parallel, I use a Gabor filter. I obtain Gabor filter responses, for 36 orientations by 19 scales. I first choose the maximum response over orientations at each scale. Then I compute the mean squared response of the results. Fig 2 shows Gabor filter responses.

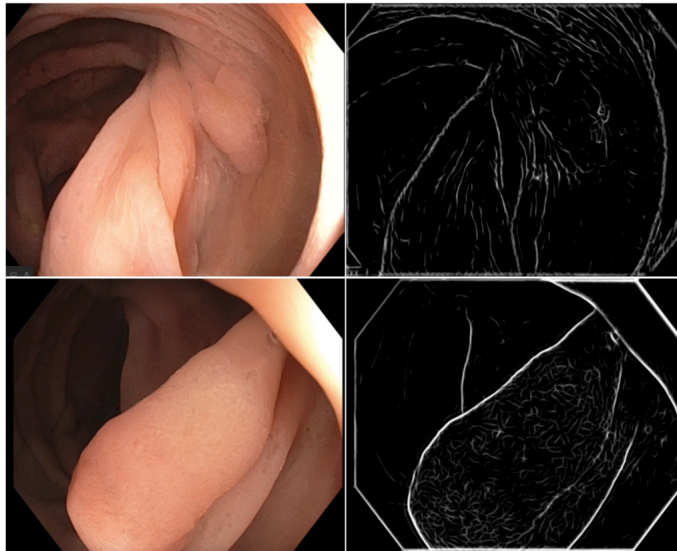


Figure 2: Colonoscopy images (left) and resulting Gabor feature maps (right).

I wish to classify those three types of edge patterns into the three categories: ridge edges, innominate grooves and random lines. I first extract ridge edges. Because ridge edges are deep, are more or less parallel and have large spacing, the Gabor filter outputs for them are brighter and longer than innominate grooves and random grooves, I can obtain these edges using thresholds on intensity and length.

Then I classify the residue of edge patterns into innominate grooves and random lines. Innominate grooves are commonly on the colon surface. They are narrow and more or less parallel with each other. I use Hough transform to detect lines. I classify edge patterns and add windows pixel by pixel. Around each pixel, I add a window which contains 3-4 lines. I calculate the difference between the maximum angle and the minimum angle in each window. If the difference is larger than 45 degrees, the window center pixel is classified into random lines. Otherwise, it is an innominate groove.

This pixel-wise classification produces reasonable results. Fig 3 top shows the pixel-wise results. Some pixels are wrongly classified. I need to refine our results. It is logical that pixels in the same line should belong to the same classification. I add a larger window than windows that I re used to detect parallel lines before. At each pixel, I count the classifications of nearby pixels lighted by decreasing functions of the distance from the center pixel. If a pixel belongs to innominate grooves, but most nearby pixels belong to random lines, this refinement step would reclassify this pixel into random lines. Fig 3 bottom compares the results of pixel-wise

classification and the results of refinement classification.

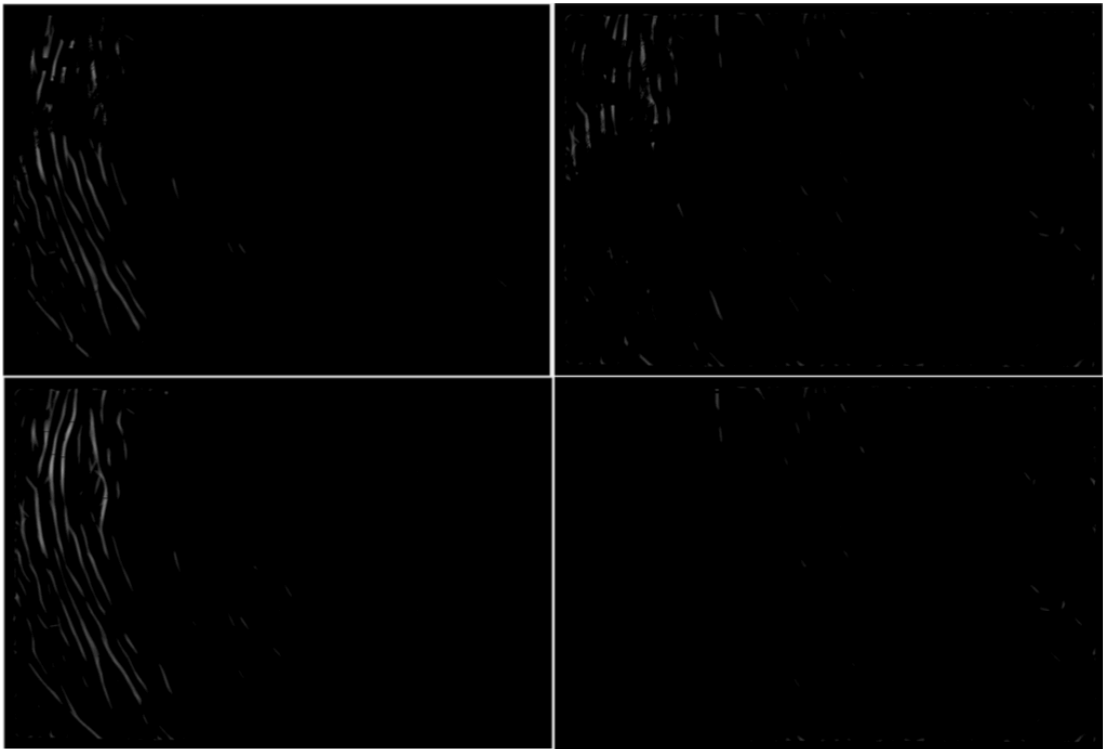


Figure 3: Initial (top) and refined (bottom) classification of lines into parallel (left) and non-parallel (right) groups

d. Results

As discussed above, random lines often indicate the presence of a flat lesion. I define a random line density as the number of random line pixels divided by the number of total pixels in the frame. A high density indicates that this region is likely to contain a flat polyp.

Random line density	mean	Std.
Polyp frame	1.13	1.13
No-polyp frame	0.42	0.32

Table 1: Mean and standard deviation of random line density

threshold	0.6	0.7	0.8
TPR (true positive ratio)	51.83%	46.36%	41.46%
FPR (false positive ratio)	26.32%	20.18%	14.04%

Table 2: TPR and FPR based on binary classification using different threshold

I use 114 no-polyp frames and 164 polyp frames to test. Table 1 summarizes the results of

this experiment. The random line density of polyp frames is relatively high than the density of no-polyp frames. Table 2 shows binary classification results using different threshold.

b). Vessel features

a. Introduction

Along with groove features, vessel features may also be valuable. There are two types of vessels useful for polyp detection:

- 1) Broad vessels, disrupted by polyps in the colon;
- 2) Narrow vessels, which not only can be twigs of broad vessels but also can unexpectedly appear inside polyps. Characteristic properties, such as tortuosity and density, of narrow vessels inside polyps are distinct from properties of narrow vessels which are twigs of broad vessels.

b. Vessel detection

The vessel detection algorithm is achieved by Linear Discriminant Analysis (LDA). While ultimate I will detect vessels automatically, I first manually labeled certain sections of vessels of an image and saved them as a mask image. Then the LDA algorithm used the mask image to train a best linear combination of input pixel intensities which separate vessels from the background. Fig 4 shows the hand labeled vessels.

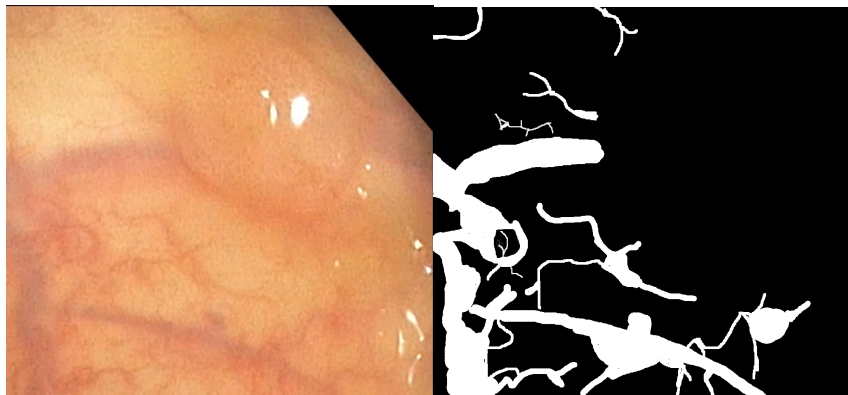


Figure 4: original frame (left) and hand labeled vessels (right)

c. vessel disruption

Vessel disruption can signal a flat polyp. Suppose I can track the vessels so that I know where the vessel is disrupted. The areas beyond disruptions are likely to contain flat polyps. If a frame contains a vessel disruption, I draw a semicircle whose center is the vessel disrupted position and whose diameter is perpendicular with the vessel direction. If this semicircle does not include any vessel pixel, it represents a high probability polyp region. I defined this semicircle as SC map. Fig 5 shows the original frame and the vessel disruption feature

extracted from it. In current stage, I do it manually.

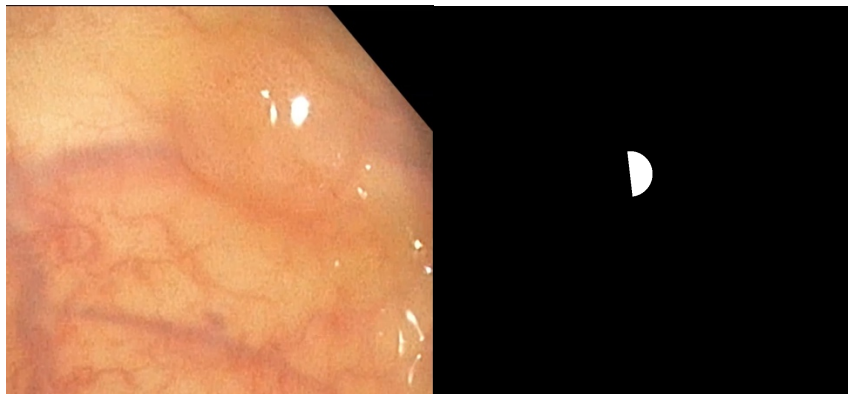


Figure 5: original frame (left) and vessel disruption (right)

d. independent narrow vessels

Frequently flat polyps contain independent narrow vessels. These are narrow vessels which are not connected to broad vessels. When some sections of narrow vessel unexpectedly appear, the region is likely to be in a flat polyp. I use the density of independent narrow vessels (INVD) as another flat polyp detection feature. The computation method of INVD map is the same as the RLD map. As shown in Fig 6, high densities of independent narrow vessels concentrate in flat polyp regions. The independent narrow vessels are labeled by myself.



Figure 6: original frame (left) and INVD (right)

e. Results

I use the same database as edge feature used. There are 24 vessel disruption frames of 114 polyp frames and no vessel disruption frames of 164 no-polyp frames.

Random line density	mean	Std.
Polyp frame	2.63	3.51
No-polyp frame	0.00	0.00

Table 3: Mean and standard deviation of INVD

threshold	0
-----------	---

TPR (true positive ratio)	83.54%
FPR (false positive ratio)	0.00%

Table 4: TPR and FPR based on binary classification using different threshold

Table 3 shows the mean and the standard deviation of INVD. The INVD value of polyp frames are relatively high. Using 0 as threshold to do a binary classification, the TPR is 83.54% and FPR is 0.88% as Table 4 showing.

c). VGG16 features

a. Feature generation

Fig 7 is a diagram illustrating the VGG16 architecture for the frame-based classification. I used the pre-trained VGG16 that is a convolutional neural network trained on more than a million images from the ImageNet database [3]. This network has learned rich feature representations for a wide range of images. As the figure showing, this architecture can use these features to classify the input image into 1000 categories. In my case, I just need to classify the input image into 2 categories, flat polyp frames and no-polyp frames. I switched the last layer with 2 outputs, froze the other part, the feature generation part of the network, and retrained the switched part using 270 no-polyp frames and 201 flat polyp frames.

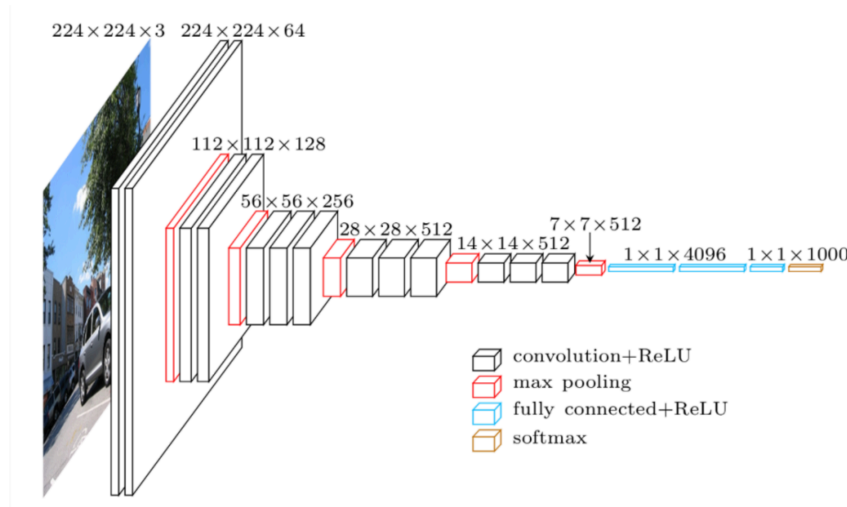


Figure 7: VGG16 architecture

b. Results

I use the same database as before. I used the difference of the two VGG16 outputs as a feature. Using 0 as the threshold, I can obtain the classification results as Table 6.

VGG16 outputs	mean	Std.
Output1	-3.00	1.61
Output2	3.75	1.83

Table 5: Mean and standard deviation of VGG16 outputs

threshold	0
TPR (true positive ratio)	93.90%
FPR (false positive ratio)	7.89%

Table 6: TPR and FPR based on binary classification using 0 threshold

2. Feature combination

I combine the features I mentioned using Linear Regression (LR), Distance Weighted Discrimination (DWD) and Bayesian Network (BN).

	Edge features			INVD	disruption	VGG16	LR	DWD	BN
threshold	0.6	0.7	0.8	0	0	0			
TPR (%)	51.83	46.36	41.46	83.54	15.85	93.90	96.34	97.56	85.37
FPR (%)	26.32	20.18	14.04	0.00	0.00	7.89	7.89	7.89	5.26

Table 7: TPR and FPR comparison

3. Conclusion

For testing we used 114 no-polyp frames and 164 flat polyp frames that contains 82 different flat polyps, including 26 sessile serrated polyps, 56 adenomas, but no hyperplastic polyps. No test frame contained a polyp that appeared in a training frame.

For DWD, the frame-based True Positive Ratio (TPR) was $78/82=97.56\%$. The frame-based False Positive ratio (FPR) was $9/114=7.9\%$. Thus, our classifier effectively detected flat polyp frames by frame-based information.

Of the 4 frames misclassified as no-polyp, one of the missed polyps was subsequently detected in other nearby frames. One polyp was completely missed perhaps because it was present in only present in one frame. The other three misclassified frames all contained the same polyp which was missed.

The polyp-based TPR was thus $80/82=97.56\%$. The TPR of sessile serrated polyps was 96.15% and the TPR of the adenomas was 98.21%. The detection rate for sessile serrated versus flat adenomas was thus not different.

The finding that serrated sessile polyps can be readily detected by our methods is important because these polyps are known to be more difficult for colonoscopists to detect.

Features, especially the INVD and VGG16, can indicate the presence of flat polyps. DWD method obtain the highest TPR. BN method lowest the FPR.

In the future, I will use atomically segmentation methods instead the hand labeled features. Our classifier gives promising results of flat polyp detection, especially when there is a sequence of frames containing the same polyp. In our experiments, we use frame-based information independently, but no sequence information. However, a frame followed the flat

polyp frame is likely to be a flat polyp frame either. In the future, we will use frame sequence as input to train our classifier, RNN for example.

Ref:

[1] N. Mayer et al., “A large dataset to train convolutional networks for disparity, optical flow, and scene flow estimation,” in Proceedings of the IEEE Conference on Computer Vision and Pattern Recognition, 2016, pp. 4040–4048.

[2] <http://global.meitu.com/>

[3] ImageNet. <http://www.image-net.org>